Intensity-independent molecular rotational decoherence lifetimes measured with mean wavelength shifts of femtosecond pulses

Hongqiang Xie (谢红强)[1,2], Guihua Li (李贵花)[3], Jinping Yao (姚金平)[2], Wei Chu (储 蔚)[2], Zhiming Chen (陈志明)[1], and Ya Cheng (程 亚)[2,4,*]

[1]*School of Science, East China University of Technology, Nanchang 330013, China*
[2]*State Key Laboratory of High Field Laser Physics, Shanghai Institute of Optics and Fine Mechanics, Chinese Academy of Sciences, Shanghai 201800, China*
[3]*School of Science, East China Jiaotong University, Nanchang 330013, China*
[4]*Collaborative Innovation Center of Extreme Optics, Shanxi University, Taiyuan 030006, China*
**Corresponding author: ya.cheng@siom.ac.cn*

Received September 3, 2018; accepted November 1, 2018; posted online November 29, 2018

We report on an experimental investigation on the dynamic decoherence process of molecular rotational wavepackets during femtosecond laser filamentation based on time-dependent mean wavelength shifts of a weak probe pulse. Details of periodic revival structures of transient alignment can be readily obtained from the measured shifted spectra due to the periodic modulation of the molecular refractive index. Using the method, we measured decoherence lifetimes of molecular rotational wavepackets in N_2 and O_2 under different experimental conditions. Our results indicate that decoherence lifetimes of molecular rotational wavepackets are primarily determined by the relative population of rotational states in the wave packet and intermolecular collisions, rather than the focusing intensity.

OCIS codes: 020.2649, 300.6530, 320.6629.
doi: 10.3788/COL201816.120201.

Molecular alignment or orientation by short intense laser pulses has been a hot research area and applied to a variety of studies, including molecular orbitals imaging, controlling high-order harmonic generation, nonlinear ultrafast spectroscopy, etc.[1–5]. During the interaction of ultrashort laser pulses with molecules, a molecular wavepacket consisting of a series of phase-locked rotational states can be produced through nonresonant Raman-type excitation[6–8]. Subsequently, during the field-free evolution, postpulse molecular alignment occurs, which leads to transient alignment of molecular wavepackets along or against the polarization direction of the pump laser field. The degree of molecular alignment is usually characterized by $\langle\langle\cos^2\theta(t)\rangle\rangle$, where θ is the angle between the molecular axis and laser polarization direction. Notably, the degree of molecular alignment cannot remain constant but will decay with time, since molecular rotational wave packets will dephase in the presence of intermolecular collisions[9–11].

So far, several optical methods have been proposed to measure the molecular alignment $\langle\langle\cos^2\theta(t)\rangle\rangle$ in the first few rotational periods (i.e., no collisions), such as the homodyne weak field polarization technique (WFPT)[12], cross-defocusing measurement[13], spatial (de)focusing effects[14], heterodyne WFPT[15,16], and a heterodyne optical method based on degenerated four wave mixing[17]. However, for long time field-free evolution (i.e., in the presence of collisions), only homodyne WFPT has been experimentally employed to detect the dynamic decoherence process of a molecular rotational wave packet via recording a homodyne signal, which is proportional to $[\langle\langle\cos^2\theta(t)\rangle\rangle - 1/3]^2$[10,11]. Obviously, the quadratic relation between recorded homodyne signals and molecular alignment $\langle\langle\cos^2\theta(t)\rangle\rangle$ obscures the positive alignment $[\langle\langle\cos^2\theta(t)\rangle\rangle > 1/3]$ and negative alignment $[\langle\langle\cos^2\theta(t)\rangle\rangle < 1/3]$.

In this work, we firstly present a simple method based on the wavelength shift (WS) of a weak probe pulse to characterize dynamic decoherence of molecular rotational wave packets. Different from measurement methods mentioned above, we detected rotational decoherence processes based on the fact that the measured WS is proportional to $\mathrm{d}\langle\langle\cos^2\theta(t)\rangle\rangle/\mathrm{d}t$, which will greatly simplify the experimental setup. Moreover, with the method, we systematically investigated the rotational decoherence of nitrogen and oxygen molecules under different experimental conditions. Specifically, we comparatively measured decoherence time of molecular rotational wavepackets under the conditions that the incident laser power is above and below the critical power for self-focusing. In addition, we also checked the dependence of molecular rotational decoherence lifetimes on gas pressures. Our results shed new light on the physical mechanisms behind decoherence dynamics of a molecular rotational wavepacket in the presence of collisions.

The propagation of intense femtosecond laser pulses in gaseous media will lead to the generation of a filament due to a dynamic balance between Kerr self-focusing and plasma defocusing[18,19]. Therefore, in general, the

refractive index of molecular gases in a filament is mainly modulated by three elements, including the Kerr effect, molecular alignment, and plasma defocusing[20–22]. The transient change of the refractive index can be expressed as

$$\Delta n(r,t) = \Delta n_{\mathrm{kerr}}(r,t) + \frac{3\pi N}{n_0}\Delta\alpha\left[\langle\langle\cos^2\theta(t)\rangle\rangle(r,t) - \frac{1}{3}\right] - \frac{2\pi e^2 N_e(r,t)}{m_e\omega_0^2}, \tag{1}$$

where the first term $\Delta n_{\mathrm{kerr}}(r,t)$ is the nonlinear Kerr index; the second term is the refractive index induced by transient molecular alignment, N is the medium density, $N \approx 2.5\times10^{19}\,\mathrm{cm}^{-3}$ at an atmospheric pressure, and $\Delta\alpha$ is the anisotropic polarizability, $\Delta\alpha_{\mathrm{N_2}} = 0.93\times10^{-24}$ cm^3 and $\Delta\alpha_{\mathrm{O_2}} = 1.14\times10^{-24}$ cm^3 for gaseous nitrogen and oxygen, respectively[23]. The last term originates from plasma's isotropic contribution, $N_e(r,t)$ is the plasma density, e is the elementary charge, and m_e is the electron mass. The first term $\Delta n_{\mathrm{kerr}}(r,t)$ is ignored because the intensity of the probe pulse in our experiments is very weak, and the cross-phase modulation only takes place near zero delay time, which is too short compared with the rotational decoherence time[24].

Therefore, the accumulated extra nonlinear phase and the WS of probe pulses in a filament are given by

$$\Delta\phi(t) = -\Delta n(t)\omega_0 L/c, \tag{2}$$

$$\Delta\lambda(t) = \Delta\lambda_{\mathrm{ma}}(t) + \Delta\lambda_{\mathrm{plasma}}(t) = \frac{L\lambda_0}{c}\frac{\mathrm{d}}{\mathrm{d}t}\Delta n(t), \tag{3}$$

where L is the filament length, $\Delta\lambda_{\mathrm{ma}}(t)$ is the WS induced by molecular alignment, and ω_0 and λ_0 are the central frequency and wavelength of the probe pulse.

The wavelength blueshift $\Delta\lambda_{\mathrm{plasma}}(t)$ caused by plasma is proportional to the time derivative of the plasma density. The WS $\Delta\lambda_{\mathrm{plasma}}(t)$ is negligible in the time window 0–200 ps according to the equation $N_e(t) = N_0/(1+bt)$, as has been reported in Ref. [25]. Finally, the amount of WS can be reasonably written as

$$\Delta\lambda(t) \approx \frac{3\pi L\lambda_0 N\Delta\alpha}{cn_0}\frac{\mathrm{d}}{\mathrm{d}t}\langle\langle\cos^2\theta(t)\rangle\rangle(r,t) = k\cdot\frac{\mathrm{d}}{\mathrm{d}t}\langle\langle\cos^2\theta(t)\rangle\rangle, \tag{4}$$

where $k = 3\pi L\lambda_0 N\Delta\alpha/cn_0$. It is worth mentioning that because of the deep spectral modulation near the revival periods, the spectra of probe pulses are not always smooth and Gaussian, which makes it difficult to directly measure the central WS. Herein, we define the mean WS (MWS) instead of the central WS as follows:

$$\Delta\lambda_{\mathrm{mws}}(\tau) = \frac{\int_\lambda \lambda\times I(\lambda)\,\mathrm{d}\lambda}{\int_\lambda I(\lambda)\mathrm{d}\lambda} - \frac{\int_{\mathrm{original\,probe}} \lambda\times I(\lambda)\,\mathrm{d}\lambda}{\int_{\mathrm{original\,probe}} I(\lambda)\,\mathrm{d}\lambda}. \tag{5}$$

τ is the time delay between the pump and probe pulses. Hence, the degree of molecular alignment can be obtained via integrating both sides of Eq. (4).

The pump–probe experimental setup is similar to that used in our previous works[26–28]. Briefly, the experiments were performed with a commercial Ti:sapphire laser system (Legend Elite Duo, Coherent, Inc.) which delivers a ~6 mJ pulse with a central wavelength of 800 nm and pulse duration of 50 fs at a repetition rate of 1 kHz. The output femtosecond laser pulses were split into two paths with a beam splitter. The first beam with a pulse energy of 2.5 mJ served as the pump. The other beam, after being frequency doubled by a 0.5-mm-thick barium borate crystal, was used as the probe. To avoid generating lasing actions with the probe pulses, the probe spectrum used in this investigation did not overlap the transition lines at 391.4 and 427.8 nm wavelengths[28,29]. A Glan–Taylor prism was inserted in the probe beam to ensure that the probe pulse was linearly polarized along the pump laser field. A motorized linear transition stage was used to precisely control the time delay between the pump and probe pulses. The zero time delay was determined by observing the beginning of plasma defocusing of the probe pulses induced by the pump pulses. The pump and probe pulses were then combined by a dichroic mirror and then focused into a gas chamber filled with nitrogen or oxygen by a 30 cm focal-length lens. After being collimated by a 20 cm focal-length lens and then passing through two dichroic mirrors (with high reflectivity at 800 nm and high transmission at 400 nm) and a neutral density filter (NDF), the spectra of probe pulses were recorded by a 1200 grooves/mm grating spectrometer (Andor Shamrock 303i).

We first examine the WSs of a 400 nm probe beam after passing through the prealigned nitrogen molecules at an atmospheric pressure rotationally excited by a 2.5 mJ, 800 nm pump pulse.

Figure 1(a) shows the temporal evolution of MWSs of the probe pulse with time delay between the pump and probe pulses. It can be seen that the amount of MWS is nearly symmetric, and the time interval of two neighboring peaks is ~8.4 ps, which is in accord with the rotational period of N_2[30]. Interestingly, the measured peak values of MWS (red dashed curve) at half or full revival time of the molecular rotational wavepacket (such as 9, 17.4, 25.73 ps…) shows an exponential decay during 0–150 ps. As shown in Fig. 1(b), at the time delay of 80.47 and 80.27 ps [marked by A and B in Fig. 1(a)], the spectra of the probe pulse were red shifted (red dotted curve) and blue shifted (blue solid curve) compared with the original probe spectrum (black dashed curve), respectively. The fine structures of MWS at the revival time as an inset was also shown in Fig. 1(b).

Figure 2(a) shows the normalized molecular alignment $\langle\langle\cos^2\theta(t)\rangle\rangle$ in the presence of intermolecular collisions deduced from the measured MWS in Fig. 1(a). It can be clearly seen that the degree of molecular alignment $\langle\langle\cos^2\theta(t)\rangle\rangle$ (black dashed curve) at half or full revival time (such as 9, 17.4, 25.73 ps…) also shows an exponential decay

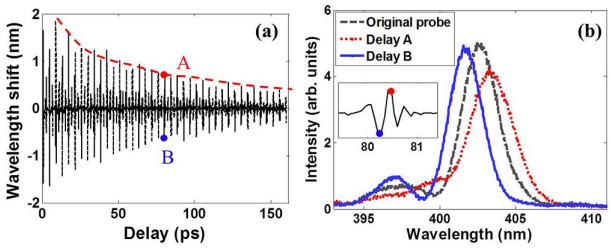

Fig. 1. (a) Mean wavelength shift (MWS) of the probe pulse as a function of the time delay between the pump and probe pulses at N_2 gas pressure of 1 bar. (b) Typical shifted spectra of the probe pulses at alignment delay of 80.47 ps (red dotted curve) and 80.27 ps (blue solid curve), respectively. The original spectrum of the probe pulse (black dashed curve) is also shown for comparison. The inset shows the detailed structure of MWS at the revival time.

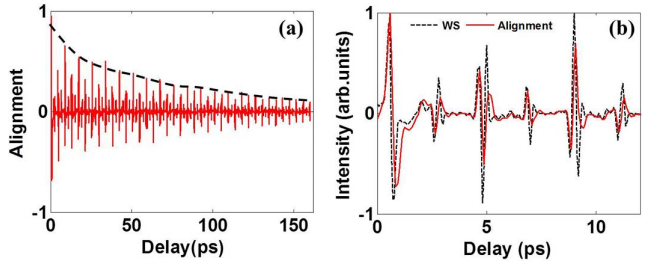

Fig. 2. (a) Deduced normalized molecular alignment $\langle\langle\cos^2\theta(t)\rangle\rangle$ from the measured result of Fig. 1(a). (b) The normalized comparison of delay-dependent MWS and molecular alignment $\langle\langle\cos^2\theta(t)\rangle\rangle$ in the time window of 0–12 ps.

during 0–150 ps, which manifests the decoherence process of the molecular rotational wavepacket. The normalized comparison of delay-dependent MWS and molecular alignment $\langle\langle\cos^2\theta(t)\rangle\rangle$ in the time window of 0–12 ps was depicted in Fig. 2(b). The peaks of MWSs are slightly earlier than the corresponding peaks of molecular alignment. According to Eq. (4), the MWS is proportional to the time derivatives of alignment factor $\langle\langle\cos^2\theta(t)\rangle\rangle$, which leads to the deviation in the peaks of MWS and molecular alignment.

According to the above experimental results, the decoherence dynamics of a molecular rotational wave packet can be faithfully encoded in shifted spectra of a weak probe laser. Therefore, using the method, we carried out the following experiments to investigate decoherence dynamics of nitrogen and oxygen molecular rotational wavepackets under different experimental conditions.

To further demonstrate the validity of our methods, we quantitatively investigated the dependence of decoherence lifetimes of molecular rotational wave packets on various gas pressures, and then we compared our results with those obtained by previous methods. The pump laser energy is set to be 2.5 mJ, and the other experimental parameters stay unchanged.

We first measured the temporal evolutions of MWSs in nitrogen at the gas pressures of 300, 700, and 1000 mbar, by which we obtained the time-dependent degrees of molecular alignment based on the measured delay-dependent MWS at the three gas pressures. To retrieve the decoherence dynamics of molecular rotational wavepackets, we plot the degree of molecular alignment as a function of multiple revival periods (i.e., 4.8, 13.2, 21.53 ps…). The results are shown in Fig. 3(a). It can be seen that for all of the gas pressures of nitrogen, the degrees of molecular alignment show an exponential decay with different lifetimes. We roughly evaluate the decoherence time (the degree of molecular alignment drops to 1/2) using the exponential fitting function $y = ae^{-b(t-c)} + d$, which is ∼110, ∼85, and ∼63 ps for the gas pressures of 300, 700, and 1000 mbar, respectively.

In addition, we carried out the same measurement on decoherence time in oxygen at various gas pressures. It can be seen from Fig. 3(b) that the degrees of molecular alignment in oxygen also show exponential decays with decoherence time of ∼93, ∼80, and ∼65 ps for the gas pressures of 300, 700, and 1000 mbar, respectively.

The decoherence time measured by MWS method is quantitatively consistent with that obtained by homodyne WFPT[10,11]. The exponential decay behaviors in Fig. 3 indicate the gradual collapse of the rotational coherent ensemble because of intermolecular collisions, and, the higher the gas pressure, the faster the exponential decay. The experimental observations can be qualitatively understood by the fact that the intermolecular collisional frequency has a quadratic dependence on gas pressure[31].

The rotational-states distribution of a wavepacket excited by femtosecond laser pulses depends on the focusing intensity distribution[32]. We perform the following experiments to study the dependence of decoherence lifetime of a molecular rotational wavepacket on the incident pump laser power.

Figures 4(a) and 4(b) show the measured decoherence lifetimes of molecular rotational wavepackets excited with femtosecond laser pulses in nitrogen and oxygen, respectively. The gas pressure was fixed at 1000 mbar. The interaction positions of the pump and probe pulses have been optimized for different incident pump intensities. Unexpectedly, it can be seen that the degree of molecular alignment at multiple revival periods shows almost the

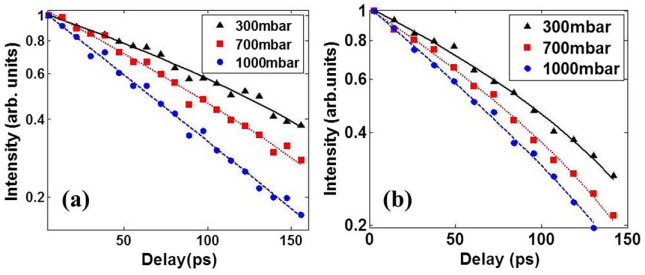

Fig. 3. Degree of molecular alignment expressed in logarithmic coordinates as a function of multiple revival periods (i.e., 4.8, 13.2, 21.53 ps…) in (a) nitrogen and (b) oxygen. The gas pressure was fixed at 300, 700, and 1000 mbar, respectively.

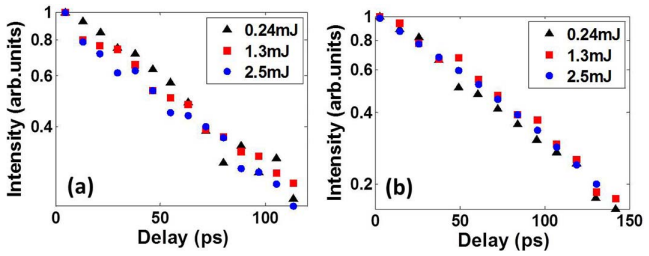

Fig. 4. Decoherence lifetimes measured with the incident pump laser energies of 0.24, 1.3, and 2.5 mJ in (a) nitrogen and (b) oxygen. The gas pressure in both cases was fixed at 1000 mbar.

same tendency for the incident pump laser energies of 0.24, 1.3, and 2.5 mJ. The decoherence lifetimes obtained at all of the pump laser energies are estimated to be $\sim 60 \pm 5$ ps, which quantitatively agrees with the results shown in Fig. 3.

To interpret the experimental observations that the decoherence lifetimes are insensitive to the pump laser energies, we first carried out the Fourier transform of the measured molecular alignment shown in Figs. 4(a) and 4(b), according to which we plot the relative population $R(J_i)$ as a function of rotational-states J_i. The results are shown in Figs. 5(a) and 5(b), respectively. The relative population of a specific rotational state is defined by $R(J_i) = P(J_i)/\sum_J P(J_i)$, where $P(J_i)$ is the absolute rotational population after the pump laser excitation. For N_2, the population of even rotational states is twice that of odd rotational states, which can be deduced from the nuclear spin statistics[30]. However, for O_2, only odd rotational states can be populated. Clearly, the relative population distribution of rotational states in molecular wavepackets is nearly the same at the three pump laser energies of 0.24, 1.3, and 2.5 mJ.

It should be stressed that the absolute population at high J (such as $J = 7, 9, 11, 13\ldots$) states in the molecular wavepackets will be larger with the increasing pump laser energy and lead to a higher degree of molecular alignment[33]. However, the relative rotational-states population remains the same with increasing pump laser energy, giving rise to almost the same decoherence lifetimes. Thus, our results indicate that decoherence lifetimes are mainly limited by the recollision and relative population of rotational states under our conditions but not the absolute population distribution in the rotational quantum states. It also indicates that extending the molecular rotational decoherence lifetime by only increasing the pump laser energies is difficult, whilst a reduction on the recollision frequency or other techniques like optical centrifuge can efficiently maintain the quantum coherence in the femtosecond laser excited rotational wavepackets.

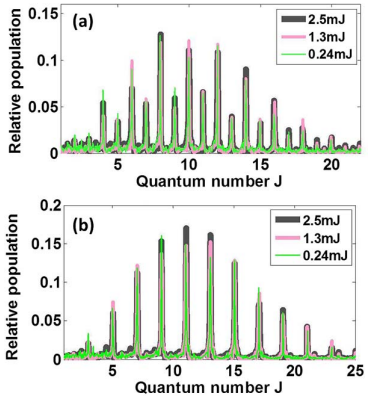

Fig. 5. Relative rotational populations of molecular rotational wave packets in (a) nitrogen and (b) oxygen are obtained via performing Fourier transforms of the corresponding curves in Figs. 4(a) and 4(b).

In conclusion, we propose a simple method to detect decoherence dynamics of molecular rotational wavepackets during femtosecond laser filamentation. The detailed revival structures of transient molecular alignment in the presence of intermolecular collisions were obtained via measuring the time-dependent MWS. Our results suggest that the decoherence lifetime of a molecular rotational wave packet is primarily determined by two factors, i.e., the relative rotational population in the wave packet and the surrounding environment. Our findings shed new light on the decoherence dynamics of molecular rotational wave packets excited with femtosecond lasers and will benefit manipulation of the coherent rotation wavepackets.

This work was supported by the National Basic Research Program of China (No. 2014CB921303), the National Natural Science Foundation of China (Nos. 61575211, 11674340, 61405220, 11404357, 61605227, 61705034, and 11704066), the Strategic Priority Research Program of Chinese Academy of Sciences (No. XDB16000000), the Key Research Program of Frontier Sciences, Chinese Academy of Sciences (No. QYZDJ-SSW-SLH010), the Shanghai Yangfan Program (No. 16YF1412700), the Natural Science Foundation of Jiangxi Province (No. 20171BAB211007), the Science and Technology Project of Jiangxi Provincial Education Department (Nos. GJJ160587 and GJJ160576), and the Shanghai Rising-Star Program (No. 17QA1404600).

References

1. J. Yao, G. Li, X. Jia, X. Hao, B. Zeng, C. Jing, W. Chu, J. Ni, H. Zhang, H. Xie, C. Zhang, Z. Zhao, J. Chen, X. Liu, Y. Cheng, and Z. Xu, Phys. Rev. Lett. **111**, 133001 (2013).
2. J. Itatani, D. Zeidler, J. Levesque, M. Spanner, D. M. Villeneuve, and P. B. Corkum, Phys. Rev. Lett. **94**, 123902 (2005).
3. O. Ghafur, A. Rouzée, A. Gijsbertsen, W. K. Siu, S. Stolte, and J. J. Vrakking, Nat. Phys. **5**, 289 (2009).
4. M. Spanner, S. Patchkovskii, E. Frumker, and P. Corkum, Phys. Rev. Lett. **109**, 113001 (2012).
5. B. Zeng, W. Chu, G. Li, J. Yao, H. Zhang, J. Ni, C. Jing, H. Xie, and Y. Cheng, Phys. Rev. A **89**, 42508 (2014).
6. T. Seideman, Phys. Rev. Lett. **83**, 4971 (1999).
7. S. Ramakrishna and T. Seideman, Phys. Rev. Lett. **95**, 113001 (2005).

8. F. Calegari, C. Vozzi, S. Gasilov, E. Benedetti, G. Sansone, M. Nisoli, S. De Silvestri, and S. Stagira, Phys. Rev. Lett. **100**, 123006 (2008).
9. S. Ramakrishna and T. Seideman, J. Chem. Phys. **124**, 034101 (2006).
10. N. Owschimikow, F. Königsmann, J. Maurer, P. Giese, A. Ott, B. Schmidt, and N. Schwentner, J. Chem. Phys. **133**, 044311 (2010).
11. T. Vieillard, F. Chaussard, D. Sugny, B. Lavorel, and O. Faucher, J. Raman Spectrosc. **39**, 694 (2008).
12. V. Renard, M. Renard, S. Guérin, Y. T. Pashayan, B. Lavorel, O. Faucher, and H. R. Jauslin, Phys. Rev. Lett. **90**, 153601 (2003).
13. V. Renard, O. Faucher, and B. Lavorel, Opt. Lett. **30**, 70 (2005).
14. Y. Feng, H. Pan, J. Liu, C. Chen, J. Wu, and H. Zeng, Opt. Express **19**, 2852 (2011).
15. A. Rouzée, V. Boudon, B. Lavorel, O. Faucher, and W. Raballand, J. Chem. Phys. **123**, 154309 (2005).
16. N. Xu, C. Wu, Y. Gao, H. Jiang, H. Yang, and Q. Gong, J. Phys. Chem. A **112**, 612 (2008).
17. X. Ren, V. Makhija, and V. Kumarappan, Phys. Rev. A **85**, 033405 (2012).
18. A. Couairon and A. Mysyrowicz, Phys. Rep. **441**, 47 (2007).
19. S. L. Chin, S. A. Hosseini, W. Liu, Q. Luo, F. Théberge, N. Akozbek, A. Becker, V. P. Kandidov, O. G. Kosareva, and H. Schroeder, Can. J. Phys. **83**, 863 (2005).
20. P. Béjot, Y. Petit, L. Bonacina, J. Kasparian, M. Moret, and J.-P. Wolf, Opt. Express **16**, 7564 (2008).
21. C. Marceau, S. Ramakrishna, S. Genier, T. Wang, Y. Chen, F. Theberge, M. Chateauneuf, J. Dubois, T. Seideman, and S. L. Chin, Opt. Commun. **283**, 2732 (2010).
22. H. Cai, J. Wu, A. Couairon, and H. Zeng, Opt. Lett. **34**, 827 (2009).
23. S. Varma, Y. Chen, and H. M. Milchberg, Phys. Plasmas **16**, 056702 (2009).
24. J. K. Wahlstrand, J. H. Odhner, E. T. McCole, Y. Cheng, J. P. Palastro, R. J. Levis, and H. M. Milchberg, Phys. Rev. A **87**, 053801 (2013).
25. J. Papeer, D. Gordon, P. Sprangle, M. Botton, and A. Zigler, Appl. Phys. Lett. **103**, 244102 (2013).
26. H. Xie, B. Zeng, G. Li, W. Chu, H. Zhang, C. Jing, J. Yao, J. Ni, Z. Wang, Z. Li, and Y. Cheng, Phys. Rev. A **90**, 042504 (2014).
27. H. Xie, G. Li, W. Chu, B. Zeng, J. Yao, C. Jing, Z. Li, and Y. Cheng, New J. Phys. **17**, 073009 (2015).
28. J. Yao, G. Li, C. Jing, B. Zeng, W. Chu, J. Ni, H. Zhang, H. Xie, C. Zhang, H. Li, H. Xu, S. L. Chin, Y. Cheng, and Z. Xu, New J. Phys. **15**, 023046 (2013).
29. G. Li, C. Jing, B. Zeng, H. Xie, J. Yao, W. Chu, J. Ni, H. Zhang, H. Xu, Y. Cheng, and Z. Xu, Phys. Rev. A **89**, 033833 (2014).
30. P. W. Dooley, I. V. Litvinyuk, K. F. Lee, D. M. Rayner, M. Spanner, D. M. Villeneuve, and P. B. Corkum, Phys. Rev. A **68**, 023406 (2003).
31. N. St. J. Braithwaite, Plasma Sources Sci. Technol. **9**, 517 (2000).
32. A. A. Milner, A. Korobenko, J. W. Hepburn, and V. Milner, Phys. Rev. Lett. **11**, 3043005 (2014).
33. P. Peng, Y. Bai, N. Li, and P. Liu, AIP Adv. **51**, 27205 (2015).